Published in final edited form as:
ACS Chem Biol. 2013 January 18; 8(1): 71–81. doi:10.1021/cb300631k.

Transition States, Analogues and Drug Development

Vern L. Schramm
Department of Biochemistry, Albert Einstein College of Medicine, 1300 Morris Park Avenue, Bronx NY 10461

Abstract

Enzymes achieve their transition states by dynamic conformational searches on the fsec to psec timescale. Mimics of reactants at enzymatic transition states bind tightly to enzymes by stabilizing the conformation optimized through evolution for transition state formation. Instead of forming the transient transition state geometry, transition state analogues convert the short-lived transition state to a stable thermodynamic state. Enzymatic transition states are understood by combining kinetic isotope effects and computational chemistry. Analogues of the transition state can bind millions of times tighter than substrates and show promise for drug development for several targets.

Keywords

Kinetic isotope effects—the experimentally observed change in reaction rate caused by a specific isotopic substitution in a reactant substrate of the enzyme. Kinetic isotope effects are largest for atoms near the bonds being broken at the transition state but can be partly or fully hidden by kinetic effects obscuring the chemical step.; **Intrinsic kinetic isotope effects**—kinetic isotope effects directly from the chemical step with all obscuring effects removed. Intrinsic kinetic isotope effects report on the bond vibrational status of the labeled reactant atom at the transition state.; **Transition state**—the traditional description is a one-dimensional energetic description: the point on the reaction coordinate profile of highest energy relative to substrate.; **Transition state analysis**—the process of measuring intrinsic kinetic isotope effects at sufficient atomic positions to permit reconstruction of a transition state wave function by computational matching of all isotope effects to a quantum chemistry-derived transition state.; **Transition state structure**—a static chemical model of the bond lengths, angles and electron density at the van der Waals surface of the reactant at the instant of the transition state. The transition state structure has a lifetime on the fsec timescale and has equal probability of partitioning to reactant or product.; **Transition state analogue**—a chemically stable molecule with features of bond lengths, angles and electron density at the van der Waals surface to resemble the actual transition state more closely than it does the reactant. Faithful mimics of enzymatic transition states bind more tightly than substrates by orders of magnitude.; **Slow protein conformational changes**—enzymes undergo loop, flap and domain motions to bind reactants and release products. These slow conformational changes are necessary steps in an enzymatic catalytic cycle but are too slow to couple to transition state formation.; **Dynamic barrier crossing**—reactants aligned in the catalytic site by the slow conformational change are subjected to local, fast interactions with catalytic site groups moving on the fsec time scale. When the interactions are optimized by simultaneous chance motion, the

vern.schramm@einstein.yu.edu.

Financial conflicts. Certain of the transition state analogue inhibitors described in this manuscript have been licensed to pharmaceutical companies for clinical development by the Albert Einstein College of Medicine. The College owns the patents and may collect milestone and royalty payments should the drug development programs be successful. The author and collaborators may benefit from the College distribution policy of proceeds on intellectual property.

barrier to the reaction falls, the transition state is reached and barrier crossing (chemical reaction) can occur.; **Heavy enzyme**—enzyme with isotopically substituted atoms to increase the protein mass and thereby decrease the bond vibrational frequency of the protein. Substitution with ^{2}H, ^{13}C and ^{15}N alters mass but not electrostatics according to the Born-Oppenheimer approximation.

Introduction

A major application of enzymatic transition state information involves the design of transition state analogues that will act as tight-binding inhibitors.[1,2] As enzymatic transition states are not well understood, we begin with a protein dynamic (but still controversial) description of the transition state. Distinctions are drawn between transition states and intermediates, transition state analogues and enzymatic intermediate analogues. Transition state analysis empowers the discovery process by providing design elements for stable chemical entities to mimic specific transition states. Tight binding of transition state analogues also involves protein dynamic motion.[3,4] Conservation of entropic components contributes to the design of tight-binding transition state analogues.[5]

A dynamic description of the transition state

The transition state in chemistry is defined by the time for atoms to move apart or together to form a new bond, and thus is known to occur on the time scale of bond vibrations.[6] Energetically, the transition state is the point on the reaction coordinate profile of highest energy relative to substrate. Direct observation of transition states have been made in the gas phase by fsec laser techniques.[7–9] The definition of the transition state is a statistical mechanics one, the point where the energetics of bond making or breaking has equal probability of moving from the transition state toward either the reactant or the product basins. Transition path sampling analysis at enzymatic catalytic sites where the motions of both local protein groups and reactants are included show that transition states formed on enzymes also have lifetimes on the fsec time scale of bond vibrations.[10–13] Motions of the surrounding amino acids vary on the fsec timescale in response to the bond vibrational modes of their individual carbon, nitrogen, oxygen and hydrogen covalent bonds. Their positions vary by approximately 0.5 Å in their thermal ellipsoids. In contrast, larger enzyme conformational changes associated with substrate binding, loop or flap motion and domain interactions are much slower, on the μsec to msec range. Slow motions are essential to provide the correct protein alignment to permit catalysis to occur, but these time scales are 10^{8} to 10^{12} slower than the lifetime of the transition state and cannot be coupled to motions associated with transition state formation. Atomic vibrations of the amino acids and reactants prior to the transition state transmit their fsec dynamic motions into a stochastic search pattern, eventually finding the geometry for transition state formation.

Thus, the function of enzymes involves at least two distinct states, a low-frequency step to find the correct backbone geometry and a high-frequency search to find the exact local geometry at the catalytic site. Klinman has called these states preorginazation and reorganization in hydride transferases.[14] How efficient is the high frequency search? On-enzyme chemistry occurs on the msec time scale. A peptide backbone structural change that takes one msec to position the Michaelis complex in an appropriate geometry to search for the transition state (the near-attack-configuration or NAC of Bruice)[15] will hold it there for a fraction of the rate constant, perhaps 100 μsec, before relaxing to the open conformation to release reactants or products. During that 100 μsec, bond vibrations with a time constant of 10 fsec can search through approximately 10^{7} distinct local conformations. One of these, occurring simultaneously with favorable interactions from neighboring catalytic site groups locates the transition state. And there is also a distinct probability that the transition state

will not be found during one slow conformational excursion. Reactants can then exchange into the solvent and enjoy several excursions into the catalytic site before this repeated process leads to barrier crossing. The relatively fast msec time scale of the overall process of binding, slow conformational change and fsec dynamic search still leads to many turnovers per sec and gives enzymes their famous catalytic rate enhancements, as much as 10^{20} relative to non-enzymatic solution chemistry.[16] In this view of dynamic enzyme chemistry, bond breaking is not slaved to either slow or fast protein vibrational modes, but both motions are required and contribute to achieve the observed chemical rates.

An experimental approach to explore fsec enzyme dynamics

Experimental observation of the short-time scale vibrational modes and their influence on enzyme chemistry can be approached by the use of heavy enzymes.[17,18] The first example of this approach was provided by human purine nucleoside phosphorylase (PNP). In this experimental approach, PNP was expressed in the presence of metabolic precursors fully substituted with stable heavy isotopes. Thus $^{2}H_2O$ replaced water, per-deuterium, per-^{13}C glucose replaced glucose and ^{15}N ammonium salts replaced natural abundance ammonium. Enzymes produced in this expression system are purified in normal water to exchange all solvent-exchangeable protons to give protein mass approximately 10% greater than the natural abundance counterpart. The value of heavy enzyme constructs is to distinguish fsec dynamics from slower conformational changes in formation of the transition state (chemical barrier crossing).

Heavy human PNP is unchanged in the steady-state kinetic parameters of k_{cat} and K_m. These parameters are governed by the slow rates of catalytic site loop motions needed to bind and release reactants on the msec timescale. Thus, the 9.9% increased protein mass made an insignificant contribution to the slow (msec) protein motions that govern steady-state kinetics. A full kinetic isotope effect analysis of heavy and light enzymes showed that intrinsic kinetic isotope effects (KIEs) are unchanged. As intrinsic KIEs are a direct manifestation of the transition state, it was concluded that the reactants in both heavy and light PNPs have the same properties at their ribocationic transition states.[17] Thus, bond vibrational motions of the reactants defining the transition state are uncoupled to the protein mass.

In contrast to these unchanged kinetic and transition state parameters, on-enzyme chemistry (the probability of barrier crossing) was slowed by approximately 30% in the heavy enzyme. PNP with increased mass has altered bond vibrational frequencies in its interactions with reactants. The increased mass reduces the number of dynamic searches made per unit time and thereby decreases the probability of finding the transition state (Fig. 1).[17]

Experiments similar to those with heavy PNP were also extended to HIV-1 protease.[18] The protease is a simpler protein with a more complex reaction mechanism. Like other di-aspartyl proteases, there are three transition states, water attack on the carbonyl carbon, protonation of the leaving group nitrogen, and peptide bond loss.[19] Transition state analysis based on kinetic isotope effects and computational chemistry has shown that partial proton transfer to the leaving group nitrogen and partial bond loss to the amide leaving group characterizes the transition state (Fig. 2).[20] Fully labeled native HIV-1 protease was 11.6% heavier than its natural abundance counterpart. Heavy HIV-1 protease showed the steady-state k_{cat} decreased by 19% and K_m increased by 38% while the single-turnover on-enzyme chemistry slowed by 58%. These relatively large effects were interpreted to indicate that fsec local protein motions are linked to barrier crossing. Here too, it was proposed that an altered sampling rate decreased the probability of barrier crossing. However, in HIV-1 protease, chemistry is linked to all rate constants so that all measured kinetic parameters

show altered constants as a result of heavy protein. As multiple proton transfers are an inherent part of this mechanism, it is possible that enzyme-mediated light particle (H^+) transfers associated with the chemistry of HIV-1 protease are more sensitive to enzyme mass dynamics than the carbon and nitrogen atoms in the reaction coordinate of PNP.

Finding transition state *structure*

From the discussion above and the knowledge that transition state lifetimes occur on the fsec timescale, any description of transition state *structure* sounds oxymoronic. Despite transition state lifetimes of a few fsec, transition state structure can be defined by a combination of intrinsic kinetic isotope effects (KIE) and computational chemistry. Transition state structure refers to the atomic nature of the transition state as a fixed object. As with all biological molecules, the features of bond geometry and electrostatics near the van der Waals surface dictate interactions with other molecules. Thus, a goal in understanding transition state structure is to define these parameters at the moment of the transition state. Kinetic isotope effects applied to enzymes have provided a robust, albeit tedious method to establish estimates of the transition state structure. The potential of KIE measurements to provide information on transition state structure has been realized for decades, as has the potential for the use of enzymatic transition state information to design transition state analogues.[21–25] The potential foreshadowed the availability of sufficient computational power to interpret multiple KIE values into viable transition state models. The approach for enzymatic transition state analysis involves 1) selection of an enzyme target with chemical features suitable for synthesis of labeled substrates, 2) synthesis of the isotopically labeled substrates or designing analytical techniques for accurate measurement of natural abundance isotope effects, 3) measure intrinsic KIEs, 4) use quantum chemical approaches to match a transition state structure with the family of intrinsic KIEs, 5) solve the wavefunction of the static model of the transition state and use it for construction of an electrostatic potential map, used as the blueprint for design of a stable mimic of the transition state, 6) apply synthetic organic chemistry to the chemical synthesis of the mimics and 7) test the proposed analogues against the target enzyme.[2,26] The experimental approaches and problems are detailed in these articles which also refer to evolving technical and computational approaches. Analysis of transition state structure has been applied to more than twenty enzymes, a few of which will be highlighted below. The approach is experimentally challenging, requiring mastery of enzymatic kinetic mechanism, isotopic synthesis, quantitative and quantum chemistry and synthetic chemistry for inhibitor production.

Transition state vs intermediate analogs, HIV protease

All enzyme reactions have transition states and some have intermediates, separated by transition states. HIV-1 protease has three transition states and two intermediates.[20] Bonds in the reaction coordinate are partial at the transition states but are equilibrated in the intermediates. Intermediates are usually bound tightly to enzymes since they tend to be high-energy, unstable states. Therefore, inhibitors designed as mimics of intermediates are also bound tightly. In the HIV-1 protease example, there are nearly a dozen FDA-approved drugs that bind tightly to the enzyme and are widely considered to be transition state analogues by virtue of having an sp^3 center to mimic the geometry of the transition state.[eg. 27] Even though they bind tightly, some with dissociation constants in the pM range, resistant strains of the protease have evolved for all inhibitors. We solved the transition state structure of both native and protease-inhibitor-resistant HIV-1 proteases.[20] Their transition states are the same (Fig. 2). Drug design that delivers faithful mimics of transition state analogues for HIV-1 protease should therefore show powerful inhibition of both native and resistant proteases. Comparisons of one of the presumed transition state analogue drugs in use for HIV-1 protease with the actual transition state reveals the drug to be an intermediate

analogue rather than a transition state analogue. These details of catalytic mechanism are important in driving next-generation chemistry for transition state analogue design.

What happens when transition state analogues bind to their targets?

The original proposal for tight binding of transition state analogues came from the Pauling proposal of tight-binding to the activated state.[28] Wolfenden gave the proposal a thermodynamic explanation by assuming that the transition state is in thermal equilibrium with all other steps in the enzymatic cycle and in that case, demonstrated that the affinity of the transition state species is proportional to the catalytic rate enhancement imposed by the enzyme.[22] With lifetimes in the fsec range, transition state species are not themally equilibrated with the enzyme. Transition path sampling (see below) shows that enzymatic transition states are not tightly bound, and only require a near-instantaneous dynamic state for barrier crossing. Slow conformational changes linked to the release of products. How then, does binding of transition state analogues differ from the actual transition state?

The transition state is formed by fsec dynamic motions occurring to place, by fast dynamic motions, all catalytic site residues in the right geometry for the few fsec it takes to cross the transition state barrier. The altered bound products are released by the next cycles of slow conformational changes. A transition state analogue fills the catalytic site and induces the slow conformational changes that normally occur to place the catalytic site in the appropriate geometry for the fsec search that would locate the transition state with normal reactants. The chemical stability of the transition state analogue prevents reaction, but mimics the transition state geometry the enzyme has been evolved to form. Instead of the simultaneous, coincident ballistic motions of amino acid side changes that form the transition state, the approaching amino acid groups form stable interactions in hydrogen bonds and ion pairs that resemble the transition state geometry in *thermodynamically stable*, rather than *dynamically transient* interactions. In complex with a transition state analogue, the interactions are thermally equilibrated, resemble the transition state and thus act to convert the dynamic features of the transition state to thermodynamic interactions. An example of these changes is the interaction of purine nucleoside phosphorylase (PNP) in comparing structures with substrate analogues and transition state analogues bound at the catalytic sites (Fig. 3). The substrates (phosphate or sulfate and purine nucleoside or analogue) are held by a constellation of weak hydrogen bonds in the Michaelis complex. When replaced by a transition state analogue, multiple new hydrogen and ionic bonds are formed, readily accounting for the approximately one-million fold tighter binding of these transition state analogues.[29,30]

The ability to form stable, thermodynamic complexes that resemble the transition state is experimentally and practically valuable. The position of catalytic site groups in complexes with transition state analogues suggest the positions of dynamic excursions leading to transition state formation (Fig. 3). Experimentally, they provide excellent structural starting points for computational chemistry, a physical starting point for reactant and protein complex in a geometry near the transition state. This information has been used to locate transition states in quantum mechanical/molecular mechanics (QM/MM) calculations of transition state dynamics.[31] Understanding transition states requires robust information near the transition state. Why? The QM calculations required to understand barrier crossing must be done on the fs time scale. If the starting point has the peptide backbone, loops or flaps distant from their required position for transition state formation, they are msec away from conformations related to the transition state. This separates them too far in computational time to be reached by QM approaches.[32,33] Dynamic QM/MM extrapolations from crystal structures with transition state analogues to mimic the transition state help in solving this problem.

Applications of transition state information

Even the earliest notions of enzymatic transition state structure proposed by Pauling suggested at the design of powerful inhibitors.[28] Natural product and synthetic chemistry soon confirmed the proposal that small molecules expected to mimic a proposed transition state were often good inhibitors.[34,35] As early as 1976, a list of 56 potential transition state analogues had been accumulated.[22] But the details of enzymatic transition states are needed to systematically design transition state analogues. This is the information provided by the combined intrinsic KIE and computational chemistry approach described above. Some examples of enzymes with ribocationic transition states follow. This approach has led to the most powerful inhibitors known for over a dozen enzymes. Only a few of the enzyme classes are summarized here and others are available from the literature.[2,36–39] Although transition state analysis is generally applicable, understanding enzymatic transition state structure is no guarantee of powerful inhibitors because of chemistry or chemical reactivity constraints (see Problems and prospects.).

AMP nucleoside hydrolase

AMP nucleoside hydrolase was an early subject for transition state analysis by the KIE approach.[40–44] AMP nucleoside hydrolase is a bacterial enzyme that converts AMP to adenine and ribose 5'-phosphate.[45] The same reaction is acid-catalyzed so the two can be compared.[41,46] A second feature of the AMP nucleoside hydrolase reaction is a feature of allosteric activation by ATP, without which, the k_{cat} is decreased by a factor of approximately 100.[47] Transition states differed for the chemical and enzymatic reactions and the transition state of the enzyme changed with allosteric activation. Based on the transition state structure, N7 protonation was identified as an important feature of the transition state. A natural product analogue of this transition state is formycin, 9-deazaadenosine, with a chemically stable ribosidic bond and N7 protonation.[48] Chemical synthesis of formycin 5'-phosphate provided a 34 nM inhibitor of this enzyme and supported the relationship between transition states from KIE as the basis for understanding transition state analogues (Fig. 4). A crystal structure of the *E. coli* AMP nucleosidase in complex with formycin 5'-phosphate confirmed Asp428 in a bidentate H-bond interaction with O6 and N7 to serve as the N7 proton donor at the transition state.[49] The proposed function of this enzyme is in regulation of the adenine nucleotide pool.[50] Genetic knockouts in *E. coli* exhibit elevated ATP levels and improved cold-survival, linking the enzyme to adenylate regulation and normal cell growth.[51,52]

Purine nucleoside phosphorylase (PNP)

Humans genetically deficient in PNP are normal at birth but develop a complete T-cell deficiency early in life and die from virus infections.[53,54] The metabolic pathways involve an inability of affected individuals to degrade 2'-deoxyguanosine (dGuo) which is converted to dGTP in activated T-cells. A biochemical rationale for dGTP accumulation is the up-regulation of 2'-deoxycytidine kinase in activated T-cells. The enzyme phosphorylates dGuo, permitting a cell-specific toxicity based on accumulation of dGTP to toxic levels specifically in dividing T-cells.[55] This finding could be used in treating T-cell disorders, provided that a sufficiently powerful PNP inhibitor could be found. Infants with 1% residual PNP activity do not suffer T-cell deficiency, thus inhibititors must be sufficiently powerful to block >99% activity. Early pharmaceutical attempts produced inhibitors with nM dissociation constants, but these were not sufficient to eliminate unwanted T-cells, nor were inhibitors from more than 30 patents attempting to target human PNP.[56] Transition state analysis revealed bovine PNP to have an early dissociative transition state.[57] A mimic of this transition state, based on electrostatic potential maps, was designed and synthesized and called Immucillin-H (Fig. 4). It was the first inhibitor synthesized to this design, and proved to be a 23 pM transition state analogue of bovine and a 56 pM inhibitor of human PNP.[58]

These analogues were approximately three-orders of magnitude better inhibitors than those designed by other methods.[56] Immucillin-H has since entered human clinical trials for T-cell leukemia.[59] It is effective against a large fraction of infant T-cell leukemia cells.[60]

The difference between 23 and 56 pM for bovine and human PNPs suggested the possibility that the enzymes might have different transition states, despite 100% conservation of catalytic site residues in contact with substrate (inosine) analogues at the catalytic sites and 87% overall amino acid identity in the human and bovine enzymes. Transition state analysis of human PNP demonstrated a fully dissociated leaving group without participation of the attacking nucleophile, to establish a fully developed S_N1, ribocation transition state.[61] The 3 Å distance between the ribocation and leaving group differs considerably from that of the 1.77 Å distance for bovine PNP. A new transition state analogue, DADMe-Immucillin-H, was designed to mimic these features (Fig. 4).[62] This transition state analogue binds tighter to human than to bovine PNP, supporting the argument that KIE-based TS-analysis is sufficient to permit the design and synthesis of powerful transition state analogues. DADMe-Immucillin-H is a 9 pM inhibitor of human PNP and has completed phase II clinical trials in combination with allopurinol for treatment of gout.[63] Gout results from the accumulation of uric acid in joints caused by excess uric acid in the blood. Uric acid is formed in humans only after the action of PNP to remove purine bases from 6-oxypurine nucleosides. Only PNP catalyzes these reactions in humans.

Another application of PNP transition state analogues is in blocking purine salvage in malaria. *Plasmodium falciparum*, the causative agent of malaria, is a purine auxotroph and can use only hypoxanthine as the physiologic precursor for purine necleotides.[64] The PNP from *P. falciparum* differs greatly from the human enzyme in being a hexamer with a decreased k_{cat} compared to the trimeric human enzyme. Transition state analogue design revealed DADMe-Immucillin-G as a 2 pM inhibitor of human PNP and a 290 pM inhibitor of the *P. falciparum* enzyme (Fig. 4).[65] The inhibitor blocks hypoxanthine salvage in cultured parasites. A major physiological test of the inhibitor is in infected Aotus primates. Only humans and other primates are susceptible to *P. falciparum* infections. Aotus develops a virulent infection with near 100% mortality unless treated. Administration of oral DADMe-Immucillin-G for 7 days reduced parasitemia levels in Aotus by >99.9%.[66] Parasites regrew in 3 to 10 days after drug was stopped, thus the treatment did not sterilize the host. In humans, the therapy is likely to be more effective. Why? The mechanism of action of DADMe-Immucillin-G is to block hypoxanthine formation, an essential metabolite for nucleic acid synthesis in the parasite. Aotus have a normal blood hypoxanthine of 40 μM while in humans hypoxanthine concentration is approximately 1 μM, making humans more suitable for this therapy than Aotus.[66]

Dynamics of PNP transition state analogue binding

Four generations of transition state analogues have been described for human PNP, and these have been analyzed for their thermodynamic binding properties. Protein and inhibitor dynamic analysis has compared for rigid analogues like Immucillin-H and more flexible analogues like DATMe-Immucillin-H in an attempt to explain why analogues with more molecular degrees of freedom bind tighter and with less entropic penalty than rigid analogues (Fig. 4).[5] The more flexible analogue, DATMe-Immucillin-H, binds to the enzyme with bidentate hydrogen bonds to a nitrogen of His257 (Fig. 2). The dynamic motion of bound inhibitor matches the range of motion of the His257 region of the protein and maintains stable interactions for the 10 nsec dynamic simulation. In contrast, Immucillin-H is too rigid to follow the dynamic motion of His257 and the hydrogen bond breaks and reforms on the nsec timescale. The increased system dynamic with DATMe-Immucillin-H translates to a lower entropic penalty for binding of the more flexible inhibitor.[5]

Methylthioadenosine phosphorylase (MTAP)

MTAP has a single function in humans, to recycle the 5'-methylthioadenosine (MTA) made in polyamine biosynthesis to S-adenosylmethionine. We reasoned that blocking MTAP would cause MTA accumulation, feedback inhibition on polyamine synthesis to the decrement of rapidly growing cancer cells. We solved the transition state of human MTAP, designed and synthesized transition state analogue inhibitors.[67,68] One of these, MTDIA, an 86 pM inhibitor of the target enzyme was found to be orally available and of low toxicity in mice (Fig. 4). Oral or intraperitoneal administration of the compound to immune deficient mice bearing human tumors causes inhibiton of cancer growth.[69,70] Inhibition of cancer growth occurs at drug concentrations that cause no apparent toxicity. This mechanism of action differs from all other approved anticancer drugs and thus might provide a novel addition to multiple drug therapies for cancer.

Ribosome Inactivating Proteins (RIPs)

Plants express specific ribosome inactivating proteins known to be among the most powerful toxins known and these toxins have been the object of inhibitor design.[71] Their mechanism of action is to enter mammalian cells, depurinate ribosomes and prevent protein synthesis. A single RIP molecule kills a mammalian cell. Linking RIPs to antibodies that recognize cancer epitopes delivers RIPs to the cancer. The approach kills cancers but has severe side effects by off-target activities on the capillary bed, causing vascular leak syndrome (VLS). Transition state analogues of RIPs are of interest as a possible rescue paradigm against this toxicity. The transition state of ricin A-chain was solved, and powerful transition state analogues designed for in vitro conditions.[72,73] A second generation of inhibitors was designed for Saporin, a related RIP that has robust catalytic activity and inhibitor action at neutral pH.[74] These compounds reflect transition state structure, are the most powerful inhibitors known for RIPs and may find utility in an new generation of cancer therapy using toxin immunochemotherapy combined with rescue paradigms based on transition state analogues. The inhibitors bind tightly to ricin A-chain and saporin leaf isozymes to stabilize the proteins to permit the first structures of ribosome inactivating proteins with oligonucleotides bound in a productive manner at the catalytic sites (Fig. 5).[75]

Methylthioadenosine nucleosidases (MTANs) and quorum sensing

Quorum sensing in bacteria was discovered in marine bacteria with luminescent responses to small molecules produced as cell density increased.[76] These molecules are called autoinducers, and cause altered gene expression pathways in sensitive bacteria. Searching for similar pathways in pathogenic bacteria has revealed quorum sensing pathways linked to pathogenicity islands in human bacterial parasites.[77] Genetic inactivation of quorum sensing pathways in pathogenic bacteria decreases their pathogenicity, thereby providing genetic validation of this pathway as a potential antibacterial target.[78–80] Despite the importance of the quorum sensing pathways in pathogenesis, they are not essential for bacterial growth. Therefore, inhibition of the quorum sensing pathways may decrease tissue damage in the host without placing selective pressure for resistance mutations in the infecting bacteria.[81] As bacterial antibiotic resistance is a major and growing medical problem, the quorum sensing pathway is an attractive candidate for the design of antibiotics that do not induce bacterial antibiotic resistance.

MTANs hydrolyze the N-ribosidic bond of methylthioadenosine and adenosylhomocysteine in quorum sensing pathways and are involved in the synthetic pathways of homoserine lactone and tetrahydrofuran autoinducer molecules in gram negative bacteria. Transition state analysis of MTANs from several bacterial species revealed two types of transition states.[82–84] One type, represented by the *E. coli* MTAN has a fully dissociated transition state (Fig. 4). Others represented by *Neisseria meningitides* MTAN have early transition

states with significant bond order remaining in the N-ribosidic bond at the transition states. Transition state analogues that mimic early and late transition states were used to distinguish the features of the transition states for other bacterial MTANs and thereby classify the MTANs from *N. meningitides* and *Helicobacter pylori* as early dissociative while those from *E. coli*, *Staphylococcus. aureus*, *Streptococcus. pneumonia* and *Klebsiella pneumoniae* have late dissociative character.[85] Transition state analogues were designed to the target MTAN enzymes in the quorum sensing pathways of gram negative bacteria, with dissociation constants as low as 47 fM (Fig. 4).[86] Transition state analogues are capable of blocking autoinducer-2 quorum sensing molecules in *Vibrio cholera* with an IC_{50} of 1 nM without inhibiting cell growth. Growth of Gram negative bacteria for 26-generations in excess MTAN transition state analogue did not induce resistance in the subsequent generations.[81] Transition state analogues against quorum sensing pathways thus have potential to reduce pathogenicity of gram negative bacteria without inducing resistance.

MTAN and menaquinone synthesis

Although most bacteria use MTANs exclusively in quorum sensing pathways and for MTA recycling to S-adenosylmethionine,[81] recent reports suggested that an MTAN was involved in the essential pathway for menaquinone biosynthesis in a few helical bacteria, including *Helicobacter pylori*.[87–89] Inhibitors designed for the MTANs in quorum sensing also inhibited the MTAN from *H. pylori* implicated in menaquinone synthesis. Tests against the growth of BuT-DADMe-ImmA (Fig. 4) against *H. pylori* showed IC90 values of <8 ng/mL, making the inhibitors more effective than amoxicillin, metronidazole or tetracycline, three antibiotics now in common use against *H. pylori*, a causative agent of stomach ulcers (Fig. 6).[90]

Problems and prospects

Does transition state analysis offer a panacea for drug design? No. Optimal targets include substitution at carbon, like the N-ribosyltransferases emphasized here. Reactants are neutral with sp^3 hybridization at the reaction center and the transition state is cationic with sp^2 hybridization. When distinguishing transition state features can be captured in stable chemistry, design of transition state analogs is optimized. Many transition states of interest, for example, phosphotransferases, can be solved by KIE and computational approaches, but chemical mimics of the PO_3 in flight at the transition state presents a chemical challenge in biologically compatible inhibitors. The same can be said for dehydrogenases, where hydride transfer at the transition state is unlikely to be easy to mimic. Even enzymes with displacement at carbon can be challenging. For example, the transition state of thymidine phosphorylase is known, but to date no tight binding inhibitors have been reported.[91,92] The crystal structure of this enzyme suggests a two-domain catalytic site that may be resistant to the dynamic transition state forces for tight binding outlined here.[93] Another class of enzymes proving difficult for transition state analog design is that with limited catalytic enhancement by the enzyme. Thus, enzymes removing the nicotinamide from NAD^+ in ADP-ribosyltransferase reactions do not bind tightly to transition state analogs, presumably because the enzymatic rate enhancement is limited.[94,95]

Despite these problems, large numbers of potential targets remain to be explored by transition state approaches. First, understanding transition state structure is a worthy goal on its own, independent of analog design considerations. Analog design is an application of transition state information, and when successful, can provide useful new inhibitors. When the optimal substitution at carbon category is considered, the array of relevant biological reactions is broad. Redesign of inhibitors for validated pharmaceutical targets is possible by understanding transition state structure. New areas for transition state exploration are the complex reactions of nucleic acid processing, post-translational modification of regulatory

proteins and epigenetic control. While the challenges are great, the potential for new knowledge is greater.

Conclusions

Knowledge of enzymatic transition states provides sufficient information to synthesize mimics that bind tightly to their cognate enzymes. Fast dynamic protein motion is important for enzymes to locate the transition state for chemical barrier crossing. Matching conformational dynamics of transition state analogues to catalytic site dynamics optimizes binding interactions. The transition state analogues provide tools for mechanistic and structural studies. Several transition state analogues designed by this method are in clinical trials, supporting the design of transition state analogues as a productive research approach to translational medical research.

Acknowledgments

Research reported here is the product of collaborative research between the V. L. Schramm laboratory and R. H. Furneaux, P. C. Tyler, G. B. Evans and other members of the Carbohydrate Chemistry Team, Industrial Research Ltd., Lower Hutt, New Zealand for design and synthesis of transition state analogue inhibitors. Structural biology collaboration is with the laboratory of S. C. Almo at the Albert Einstein College of Medicine. Quantum computational chemistry is in collaboration with the laboratory of S. D. Schwartz at the Albert Einstein College of Medicine and now at the University of Arizona. Molecular mechanics dynamic simulations have been in collaboration with C. L. Brooks III, at the University of Michigan. Finally, the talented postdoctoral fellows and students whose names appear on the publications are the agents of accomplishment for all work reported here.

Support for this work has been provided by NIH research grants GM41916 for transition state analysis, AI049512 and Medicines for Malaria for research in malaria, CA072444 for research in ribosome inactivating proteins, CA135405 for the study of MTAP as an anticancer target, and program project GM068036 for the study of dynamic contributions to catalysis.

References

1. Wolfenden R. Conformational aspects of inhibitor design: enzyme-substrate interactions in the transition state. Bioorg. Med. Chem. 1999; 7:647–652. [PubMed: 10400319]
2. Schramm VL. Enzymatic transition states, transition-state analogs, dynamics, thermodynamics, and lifetimes. Annu. Rev. Biochem. 2011; 80:703–732. [PubMed: 21675920]
3. Saen-Oon S, Quaytman-Machleder S, Schramm VL, Schwartz SD. Atomic detail of chemical transformation at the transition state of an enzymatic reaction. Proc. Natl. Acad. Sci. U. S. A. 2008; 105:16543–16548. [PubMed: 18946041]
4. Schwartz SD, Schramm VL. Enzymatic transition states and dynamic motion in barrier crossing. Nat. Chem. Biol. 2009; 5:551–558. [PubMed: 19620996]
5. Hirschi JS, Arora K, Brooks CL 3rd, Schramm VL. Conformational dynamics in human purine nucleoside phosphorylase with reactants and transition-state analogues. J. Phys. Chem. B. 2010; 114:16263–16272. [PubMed: 20936808]
6. Zewail AH. Femtochemistry: Atomic-scale dynamics of the chemical bond using ultrafast lasers (Nobel Lecture). Angew. Chem., Int. Ed. Engl. 2000; 39:2586–2631. [PubMed: 10934390]
7. Dantus M, Bowman RM, Baskin JS, Zewail AH. Femtosecond real-time alignment in chemical reactions. Chem. Phys. Lett. 1989; 159:406–412.
8. Pedersen S, Bañares L, Zewail AH. Femtosecond vibrational transition-state dynamics in a chemical reaction. J. Chem. Phys. 1992; 97:8801–8804.
9. Polanyi JC, Zewail AH. Direct observation of the transition state. Acc. Chem. Res. 1995; 28:119–132.
10. Bolhuis PG, Chandler D, Dellago C, Geissler PL. Transition path sampling: throwing ropes over rough mountain passes in the dark. Annu. Rev. Phys. Chem. 2002; 53:291–318. [PubMed: 11972010]

11. Dellago C, Bolhuis PG, Chandler D. Efficient transition path sampling: application to Lennard-Jones cluster rearrangements. J. Chem. Phys. 1998; 108:9236–9245.
12. Basner JE, Schwartz SD. How enzyme dynamics helps catalyze a chemical reaction in atomic detail: a transition path sampling study. J. Am. Chem. Soc. 2005; 127:13822–13831. [PubMed: 16201803]
13. Antoniou D, Schwartz SD. Protein dynamics and enzymatic chemical barrier passage. J. Phys. Chem. B. 2011; 115:15147–15158. [PubMed: 22031954]
14. Nagel ZD, Klinman JP. A 21st century revisionist's view at a turning point in enzymology. Nat. Chem. Biol. 2009; 5:543–550. [PubMed: 19620995]
15. Hur S, Bruice TC. Just a near attack conformer for catalysis (chorismate to prephenate rearrangements in water, antibody, enzymes, and their mutants). J. Am. Chem. Soc. 2003; 125:10540–10542. [PubMed: 12940735]
16. Wolfenden R. Benchmark reaction rates, the stability of biological molecules in water, and the evolution of catalytic power in enzymes. Annu. Rev. Biochem. 2011; 80:645–667. [PubMed: 21495848]
17. Silva RG, Murkin AS, Schramm VL. Femtosecond dynamics coupled to chemical barrier crossing in a Born-Oppenheimer enzyme. Proc. Natl. Acad. Sci. USA. 2011; 108:18661–18665. [PubMed: 22065757]
18. Kipp DR, Silva RG, Schramm VL. Mass-dependent bond vibrational dynamics influence catalysis by HIV-1 protease. J. Am. Chem. Soc. 2011; 133:19358–19361. [PubMed: 22059645]
19. Shen CH, Tie Y, Yu X, Wang YF, Kovalevsky AY, Harrison RW, Weber IT. Capturing the reaction pathway in near-atomic-resolution crystal structures of HIV-1 protease. Biochemistry. 2012; 51:7726–7732. [PubMed: 22963370]
20. Kipp DR, Hirschi JS, Wakata A, Goldstein H, Schramm VL. Transition states of native and drug-resistant HIV-1 protease are the same. Proc. Natl. Acad. Sci. USA. 2012; 109:6543–6548. [PubMed: 22493227]
21. Cleland WW. Isotope effects: determination of enzyme transition state structure. Methods Enzymol. 1995; 249:341–373. [PubMed: 7791618]
22. Wolfenden R. Transition state analog inhibitors and enzyme catalysis. Annu Rev Biophys Bioeng. 1976; 5:271–306. [PubMed: 7991]
23. Wolfenden R. Transition state analogues for enzyme catalysis. Nature. 1969; 223:704–705. [PubMed: 4979456]
24. Gandour, RD.; Schowen, RL. Transition states of biochemical processes. Plenum Press; NY: 1978.
25. Cleland, WW.; O'Leary, MH.; Northrop, DB. Isotope effects on enzyme-catalyzed reactions. Proceedings of the Sixth Annual Harry Steenbock Symposium; University Park Press; 1977.
26. Schramm VL. Enzymatic transition-sate analysis and transition-state analogs. Methods Enzymol. 1999; 308:301–355. [PubMed: 10507010]
27. Mahalingam AK, Axelsson L, Ekegren JK, Wannberg J, Kihlström J, Unge T, Wallberg H, Samuelsson B, Larhed M, Hallberg A. HIV-1 protease inhibitors with a transition-state mimic comprising a tertiary alcohol: improved antiviral activity in cells. J Med Chem. 2010; 53:607–615. [PubMed: 19961222]
28. Pauling L. Chemical achievement and hope for the future. Am Sci. 1948; 36:51–58. [PubMed: 18920436]
29. Fedorov A, Shi W, Kicska G, Fedorov E, Tyler PC, Furneaux RH, Hanson JC, Gainsford GJ, Larese JZ, Schramm VL, Almo SC. Transition state structure of purine nucleoside phosphorylase and principles of atomic motion in enzymatic catalysis. Biochemistry. 2001; 40:853–860. [PubMed: 11170405]
30. Schramm VL, Shi W. Atomic motion in enzymatic reaction coordinates. Curr. Opin. Struct. Biol. 2001; 11:657–665. [PubMed: 11751045]
31. Ferrer S, Ruiz-Pernía J, Martí S, Moliner V, Tuñón I, Bertrán J, Andrés J. Hybrid schemes based on quantum mechanics/molecular mechanics simulations goals to success, problems, and perspectives. Adv. Protein Chem. Struct. Biol. 2011; 85:81–142. [PubMed: 21920322]

32. Exequiel JR, Pineda T, Antoniou D, Schwartz SD. Slow conformational motions that favor sub-picosecond motions important for catalysis. J. Phys. Chem. B. 2010; 114:15985–15990. [PubMed: 21077591]
33. Garcia-Viloca M, Gao J, Karplus M, Truhlar DG. How enzymes work: analysis by modern rate theory and computer simulations. Science. 2004; 303:186–195. [PubMed: 14716003]
34. Sawa T, Fukagawa Y, Homma I, Takeuchi T, Umezawa H. Mode of inhibition of coformycin on adenosine deaminase. J. Antibiot. (Tokyo). 1967; 20:227–231. [PubMed: 6072897]
35. Cha S, Agarwal RP, Parks RE Jr. Tight-binding inhibitors-II. Non-steady state nature of inhibition of milk xanthine oxidase by allopurinol and alloxanthine and of human erythrocytic adenosine deaminase by coformycin. Biochem. Pharmacol. 1975; 24:2187–2197. [PubMed: 1212267]
36. Guan R, Ho MC, Fröhlich RF, Tyler PC, Almo SC, Schramm VL. Methylthioadenosine deaminase in an alternative quorum sensing pathway in *Pseudomonas aeruginosa*. Biochemistry. 2012; 51:9094–9103.
37. Thomas K, Haapalainen AM, Burgos ES, Evans GB, Tyler PC, Gulab S, Guan R, Schramm VL. Femtomolar inhibitors bind to 5'-methylthioadenosine nucleosidases with favorable enthalpy and entropy. Biochemistry. 2012; 51:7541–7550.
38. Wang S, Haapalainen AM, Yan F, Du Q, Tyler PC, Evans GB, Rinaldo-Matthis A, Brown RL, Norris GE, Almo SC, Schramm VL. A picomolar transition state analogue inhibitor of MTAN as a specific antibiotic for Helicobacter pylori. Biochemistry. 2012; 51:6892–6894. [PubMed: 22891633]
39. Clinch K, Evans GB, Fröhlich RF, Gulab SA, Gutierrez JA, Mason JM, Schramm VL, Tyler PC, Woolhouse AD. Transition state analogue inhibitors of human methylthioadenosine phosphorylase and bacterial methylthioadenosine/S-adenosylhomocysteine nucleosidase incorporating acyclic ribooxacarbenium ion mimics. Bioorg. Med. Chem. 2012; 20:5181–5187. [PubMed: 22854195]
40. Parkin DW, Schramm VL. Effects of allosteric activation on the primary and secondary kinetic isotope effects for three AMP nucleosidases. J. Biol. Chem. 1984; 259:9418–25. [PubMed: 6378909]
41. Mentch F, Parkin DW, Schramm VL. Transition-state structures for N-glycoside hydrolysis of AMP by acid and by AMP nucleosidase in the presence and absence of allosteric activator. Biochemistry. 1987; 26:921–930. [PubMed: 3552038]
42. Parkin DW, Schramm VL. Catalytic and allosteric mechanism of AMP nucleosidase from primary, beta-secondary, and multiple heavy atom kinetic isotope effects. Biochemistry. 1987; 26:913–920. [PubMed: 3552037]
43. Parkin DW, Mentch F, Banks GA, Horenstein BA, Schramm VL. Transition-state analysis of a V_{max} mutant of AMP nucleosidase by the application of heavy-atom kinetic isotope effects. Biochemistry. 1991; 30:4586–4594. [PubMed: 2021651]
44. Ehrlich JI, Schramm VL. Electrostatic potential surface analysis of the transition state for AMP nucleosidase and for formycin 5'-phosphate, a transition-state inhibitor. Biochemistry. 1994; 33:8890–8896. [PubMed: 8043576]
45. Hurwitz J, Heppel LA, Horecker BL. The enzymatic cleavage of adenylic acid to adenine and ribose 5-phosphate. J. Biol. Chem. 1957; 226:525–540. [PubMed: 13428783]
46. McCann JA, Berti PJ. Transition state analysis of acid-catalyzed dAMP hydrolysis. J. Am. Chem. Soc. 2007; 129:7055–7064. [PubMed: 17497857]
47. Schramm VL. Comparison of initial velocity and binding data for allosteric adenosine monophosphate nucleosidase. J. Biol. Chem. 1976; 251:3417–3424. [PubMed: 931993]
48. DeWolf WE Jr. Fullin FA, Schramm VL. The catalytic site of AMP nucleosidase. Substrate specificity and pH effects with AMP and formycin 5'-PO4. J. Biol. Chem. 1979; 254:10868–10875. [PubMed: 40976]
49. Zhang Y, Cottet SE, Ealick SE. Structure of *Escherichia coli* AMP nucleosidase reveals similarity to nucleoside phosphorylases. Structure. 2004; 12:1383–1394. [PubMed: 15296732]
50. Leung H,B, Schramm VL. Adenylate degradation in Escherichia coli. The role of AMP nucleosidase and properties of the purified enzyme. J. Biol. Chem. 1980; 255:10867–10874. [PubMed: 7000783]

51. Morrison BA, Shain DH. An AMP nucleosidase gene knockout in *Escherichia coli* elevates intracellular ATP levels and increases cold tolerance. Biol. Lett. 2008; 4:53–56. [PubMed: 18029299]
52. Parry BR, Shain DH. Manipulations of AMP metabolic genes increase growth rate and cold tolerance in *Escherichia coli*: implications for psychrophilic evolution. Mol. Biol. Evol. 2011; 28:2139–2145. [PubMed: 21300985]
53. Giblett ER, Ammann AJ, Wara DW, Sandman R, Diamond LK. Nucleoside-phosphorylase deficiency in a child with severely defective T-cell immunity and normal B-cell immunity. Lancet. 1975; 1:1010–1013. [PubMed: 48676]
54. Cohen A, Doyle D, Martin DW Jr. Ammann AJ. Abnormal purine metabolism and purine overproduction in a patient deficient in purine nucleoside phosphorylase. New Engl. J. Med. 1976; 295:1449–1454. [PubMed: 825775]
55. Cohen A, Gudas LJ, Ammann AJ, Staal GE, Martin DW Jr. Deoxyguanosine triphosphate as a possible toxic metabolite in the immunodeficiency associated with purine nucleoside phosphorylase deficiency. J. Clin. Invest. 1978; 61:1405–1409. [PubMed: 96138]
56. Morris PE Jr. Omura GA. Inhibitors of the enzyme purine nucleoside phosphorylase as potential therapy for psoriasis. Curr. Pharm. Des. 2000; 6:943–959. [PubMed: 10828318]
57. Kline PC, Schramm VL. Purine nucleoside phosphorylase. Catalytic mechanism and transition-state analysis of the arsenolysis reaction. Biochemistry. 1993; 32:13212–13219. [PubMed: 8241176]
58. Miles RW, Tyler PC, Furneaux RH, Bagdassarian CK, Schramm VL. One-third-the-sites transition-state inhibitors for purine nucleoside phosphorylase. Biochemistry. 1998; 37:8615–8621. [PubMed: 9628722]
59. Balakrishnan K, Verma D, O'Brien S, Kilpatrick JM, Chen Y, Tyler BF, Bickel S, Bantia S, Keating MJ, Kantarjian H, Gandhi V, Ravandi F. Phase 2 and pharmacodynamic study of oral forodesine in patients with advanced, fludarabine-treated chronic lymphocytic leukemia. Blood. 2010; 116:886–892. [PubMed: 20427701]
60. Homminga I, Zwaan CM, Manz CY, Parker C, Bantia S, Smits WK, Higginbotham F, Pieters R, Meijerink JP. In vitro efficacy of forodesine and nelarabine (ara-G) in pediatric leukemia. Blood. 2011; 118:2184–2190. [PubMed: 21730354]
61. Lewandowicz A, Schramm VL. Transition state analysis for human and *Plasmodium falciparum* purine nucleoside phosphorylases. Biochemistry. 2004; 43:1458–1468. [PubMed: 14769022]
62. Evans GB, Furneaux RH, Lewandowicz A, Schramm VL, Tyler PC. Synthesis of second-generation transition state analogues of human purine nucleoside phosphorylase. J. Med. Chem. 2003; 46:5271–5276. [PubMed: 14613329]
63. Bantia, S.; Harman, L.; Hollister, A.; Pearson, P. BCX4208, a novel enzyme inhibitor for chronic management of gout shows a low risk of potential drug-drug interactions. Presented at the Annual European Congress of Rheumatology (EULAR); Berlin, Germany. 2012 June 6–9; 2012Abstract
64. Kicska GA, Tyler PC, Evans GB, Furneaux RH, Schramm VL, Kim K. Purine-less death in *Plasmodium falciparum* induced by immucillin-H, a transition state analogue of purine nucleoside phosphorylase. J. Biol. Chem. 2002; 277:3226–3231. [PubMed: 11706018]
65. Luo M, Singh V, Taylor EA, Schramm VL. Transition-state variation in human, bovine, and *Plasmodium falciparum* adenosine deaminases. J. Am. Chem. Soc. 2007; 129:8008–8017. [PubMed: 17536804]
66. Cassera MB, Hazleton KZ, Merino EF, Obaldia N 3rd, Ho MC, Murkin AS, DePinto R, Gutierrez JA, Almo SC, Evans GB, Babu YS, Schramm VL. *Plasmodium falciparum* parasites are killed by a transition state analogue of purine nucleoside phosphorylase in a primate animal model. PLoS One. 2011; 6:e26916. [PubMed: 22096507]
67. Singh V, Schramm VL. Transition-state structure of human 5'-methylthioadenosine phosphorylase. J. Am. Chem. Soc. 2006; 128:14691–14696. [PubMed: 17090056]
68. Evans GB, Furneaux RH, Schramm VL, Singh V, Tyler PC. Targeting the polyamine pathway with transition-state analogue inhibitors of 5'-methylthioadenosine phosphorylase. J. Med. Chem. 2004; 47:3275–3281. [PubMed: 15163207]

69. Basu I, Cordovano G, Das I, Belbin TJ, Guha C, Schramm VL. A transition state analogue of 5'-methylthioadenosine phosphorylase induces apoptosis in head and neck cancers. J. Biol. Chem. 2007; 282:21477–21486. [PubMed: 17548352]
70. Basu I, Locker J, Cassera MB, Belbin TJ, Merino EF, Dong X, Hemeon I, Evans GB, Guha C, Schramm VL. Growth and metastases of human lung cancer are inhibited in mouse xenografts by a transition state analogue of 5'-methylthioadenosine phosphorylase. J. Biol. Chem. 2011; 286:4902–4911. [PubMed: 21135097]
71. Wahome PG, Robertus JD, Mantis NJ. Small-molecule inhibitors of ricin and Shiga toxins. Curr Top Microbiol Immunol. 2012; 357:179–207. [PubMed: 22006183]
72. Chen X-Y, Berti PJ, Schramm VL. Transition state analysis for depurination of DNA by Ricin A-chain. J. Am. Chem. Soc. 2000; 122:6527–6534.
73. Sturm MB, Roday S, Schramm VL. Circular DNA and DNA/RNA hybrid molecules as scaffolds for ricin inhibitor design. J. Am. Chem. Soc. 2007; 129:5544–5550. [PubMed: 17417841]
74. Sturm MB, Tyler PC, Evans GB, Schramm VL. Transition state analogues rescue ribosomes from saporin-L1 ribosome inactivating protein. Biochemistry. 2009; 48:9941–9948. [PubMed: 19764816]
75. Ho MC, Sturm MB, Almo SC, Schramm VL. Transition state analogues in structures of ricin and saporin ribosome-inactivating proteins. Proc. Natl. Acad. Sci. USA. 2009; 106:20276–20281. [PubMed: 19920175]
76. Nealson K, Platt T, Hastings JW. The cellular control of the synthesis and activity of the bacterial luminescent system. Journal of Bacteriology. 1970; 104:313–322. [PubMed: 5473898]
77. Kepseu WD, Van Gijsegem F, Sepulchre JA. Modelling the onset of virulence in pathogenic bacteria. Methods Mol. Biol. 2012; 804:501–517. [PubMed: 22144169]
78. Choi J, Shin D, Kim M, Park J, Lim S, Ryu S. LsrR-mediated quorum sensing controls invasiveness of *Salmonella typhimurium* by regulating SPI-1 and flagella genes. PLoS One. 2012; 7:e37059. [PubMed: 22623980]
79. Liang H, Deng X, Ji Q, Sun F, Shen T, He C. The *Pseudomonas aeruginosa* global regulator VqsR directly inhibits QscR to control quorum-sensing and virulence gene expression. J. Bacteriol. 2012; 194:3098–3108. [PubMed: 22505688]
80. Ulrich RL, Deshazer D, Brueggemann EE, Hines HB, Oyston PC, Jeddeloh JA. Role of quorum sensing in the pathogenicity of *Burkholderia pseudomallei*. J. Med. Microbiol. 2004; 53:1053–1064. [PubMed: 15496380]
81. Gutierrez JA, Crowder T, Rinaldo-Matthis A, Ho MC, Almo SC, Schramm VL. Transition state analogs of 5'-methylthioadenosine nucleosidase disrupt quorum sensing. Nat. Chem. Biol. 2009; 5:251–257. [PubMed: 19270684]
82. Singh V, Lee JE, Núñez S, Howell PL, Schramm VL. Transition state structure of 5'-methylthioadenosine/S-adenosylhomocysteine nucleosidase from *Escherichia coli* and its similarity to transition state analogues. Biochemistry. 2005; 44:11647–11659. [PubMed: 16128565]
83. Singh V, Schramm VL. Transition-state analysis of *S. pneumoniae* 5'-methylthioadenosine nucleosidase. J. Am. Chem. Soc. 2007; 129:2783–2795. [PubMed: 17298059]
84. Singh V, Luo M, Brown RL, Norris GE, Schramm VL. Transition-state structure of *Neisseria meningitides* 5'-methylthioadenosine/S-adenosylhomocysteine nucleosidase. J. Am. Chem. Soc. 2007; 129:13831–13833. [PubMed: 17956098]
85. Gutierrez JA, Luo M, Singh V, Li L, Brown RL, Norris GE, Evans GB, Furneaux RH, Tyler PC, Painter GF, Lenz DH, Schramm VL. Picomolar inhibitors as transition-state probes of 5'-methylthioadenosine nucleosidases. ACS Chem Biol. 2007; 2:725–734. [PubMed: 18030989]
86. Singh V, Evans GB, Lenz DH, Mason JM, Clinch K, Mee S, Painter GF, Tyler PC, Furneaux RH, Lee JE, Howell PL, Schramm VL. Femtomolar transition state analogue inhibitors of 5'-methylthioadenosine/S-adenosylhomocysteine nucleosidase from *Escherichia coli*. J. Biol. Chem. 2005; 280:18265–18273. [PubMed: 15749708]
87. Li X, Apel D, Gaynor EC, Tanner ME. 5'-methylthioadenosine nucleosidase is implicated in playing a key role in a modified futalosine pathway for menaquinone biosynthesis in *Campylobacter jejuni*. J. Biol. Chem. 2011; 286:19392–19398. [PubMed: 21489995]

88. Hiratsuka T, Furihata K, Ishikawa J, Yamashita H, Itoh N, Seto H, Dairi T. An alternative menaquinone biosynthetic pathway operating in microorganisms. Science. 2008; 321:1670–1673. [PubMed: 18801996]

89. Dairi T. Menaquinone biosyntheses in microorganisms. Methods Enzymol. 2012; 515:107–22. [PubMed: 22999172]

90. Wang S, Haapalainen AM, Yan F, Du Q, Tyler PC, Evans GB, Rinaldo-Matthis A, Brown RL, Norris GE, Almo SC, Schramm VL. A picomolar transition state analogue inhibitor of MTAN as a specific antibiotic for *Helicobacter pylori*. Biochemistry. 2012; 51:6892–4. [PubMed: 22891633]

91. Schwartz PA, Vetticatt MJ, Schramm VL. Transition state analysis of the arsenolytic depyrimidination of thymidine by human thymidine phosphorylase. Biochemistry. 2011; 50:1412–1420. [PubMed: 21222488]

92. Schwartz PA, Vetticatt MJ, Schramm VL. Transition state analysis of thymidine hydrolysis by human thymidine phosphorylase. J. Am. Chem. Soc. 2010; 132:13425–13433. [PubMed: 20804144]

93. Norman RA, Barry ST, Bate M, Breed J, Colls JG, Ernill RJ, Luke RW, Minshull CA, McAlister MS, McCall EJ, McMiken HH, Paterson DS, Timms D, Tucker JA, Pauptit RA. Crystal structure of human thymidine phosphorylase in complex with a small molecule inhibitor. Science. 2004; 12:75–84.

94. Zhou GC, Parikh SL, Tyler PC, Evans GB, Furneaux RH, Zubkova OV, Benjes PA, Schramm VL. Inhibitors of ADP-ribosylating bacterial toxins based on oxacarbenium ion character at their transition states. J. Am. Chem. Soc. 2004; 126:5690–5698. [PubMed: 15125661]

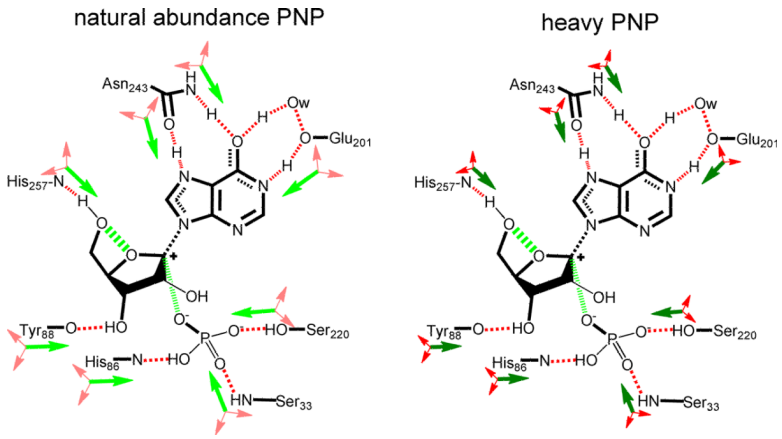

Fig. 1.

Dynamic motion in natural abundance and heavy PNPs. The green arrows show chemistry-promoting bond vibrational frequency in natural abundance (left) and heavy (right) PNPs. The natural abundance enzyme has higher frequency bond vibrations (longer light green arrows) that those in heavy PNP (shorter dark green arrows). Lower frequency bond vibrations extrapolate to fewer stochastic searches for the transition state per unit time. Bond vibrations orthogonal to the reaction coordinate and shown in red and do are non-productive bond vibrations that do not contribute to barrier crossing. The transition state is characterized by a fully-formed ribocation with minimal bonding to the oxygen of the attacking phosphate nucleophile, an event following the transition state formation. From reference 17 with permission of the publisher.

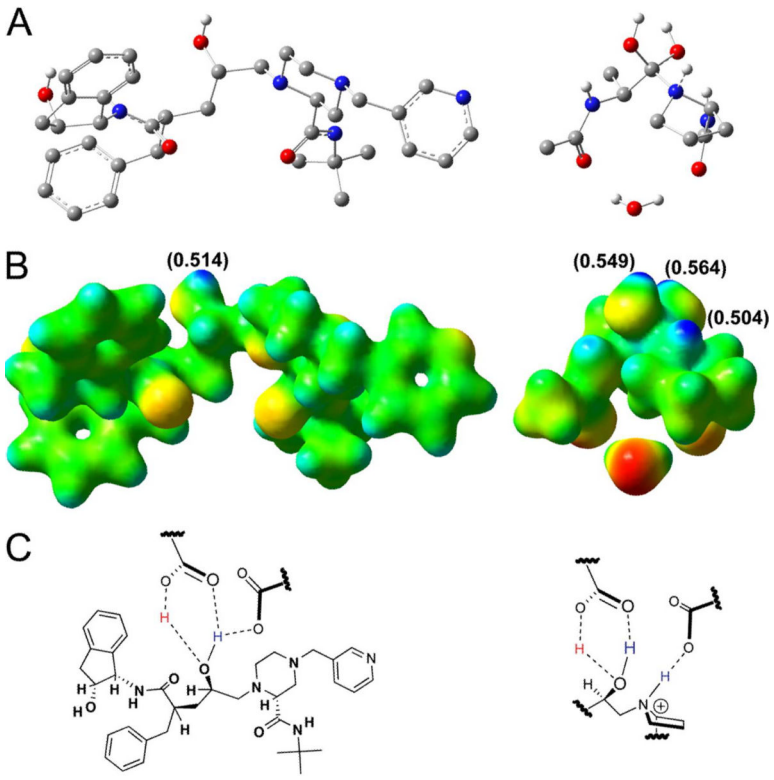

Fig. 2.

Transition state structure for HIV protease in comparison to a clinical inhibitor, indinavir. (A) The structure of bound indinavir in HIV-1 protease (PDB 2AVO, left panel). The transition state structure for the enzyme determined from intrinsic kinetic isotope effects and quantum chemistry are shown in the right panel. In B, the molecular electrostatic potential surface for indinavir is shown and compared to the transition state structure determined for HIV-1 protease (right). Natural bond order charges are indicated in parentheses (blue = electron deficient; red = electron rich). In panel C, the hydrogen bond patterns from the catalytic Asp groups are shown. From reference 20 with permission of the publisher.

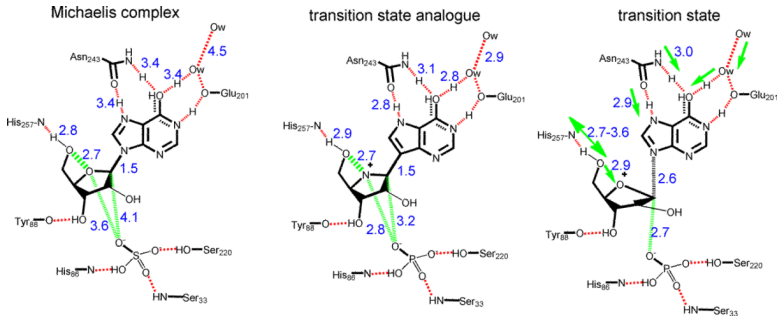

Fig. 3.

Comparing complexes in mammalian PNPs. The crystallographic structures of the Michaelis complex (left) with inosine and sulfate is compared to Immucillin-H and phosphate (middle) for bovine PNP.[29] Distances (in blue, Å) are between heavy atoms. The transition state structure (right) is taken from transition path sampling computations for barrier crossing with human PNP using guanosine as substrate.[3] Only the inosine atoms and relevant protein groups are shown for comparison with the other complexes. Green arrows show chemistry-promoting bond motions. Note that the leaving group interactions to Asn243 are similar between the transition state analogue and the transition state. In this excursion to form the transition state, the N of His257 is in motion and moves from 3.6 to 2.7 Å in the 20 fsec period including the transition state.[3]

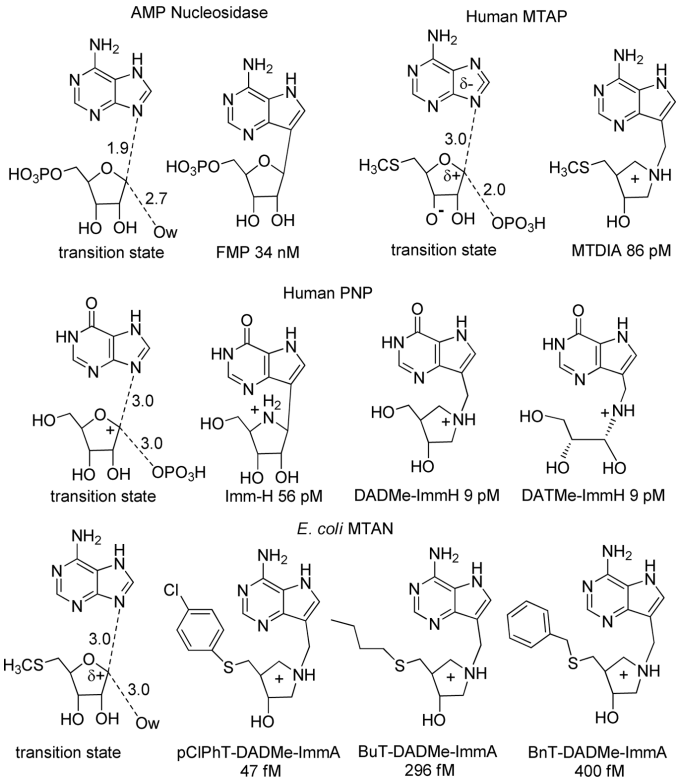

Fig. 4.

Transition states for four N-ribosyltransferases and transition state analogues. Bond lengths shown for transition states are in Å. Values shown for the inhibitors are dissociation constants.

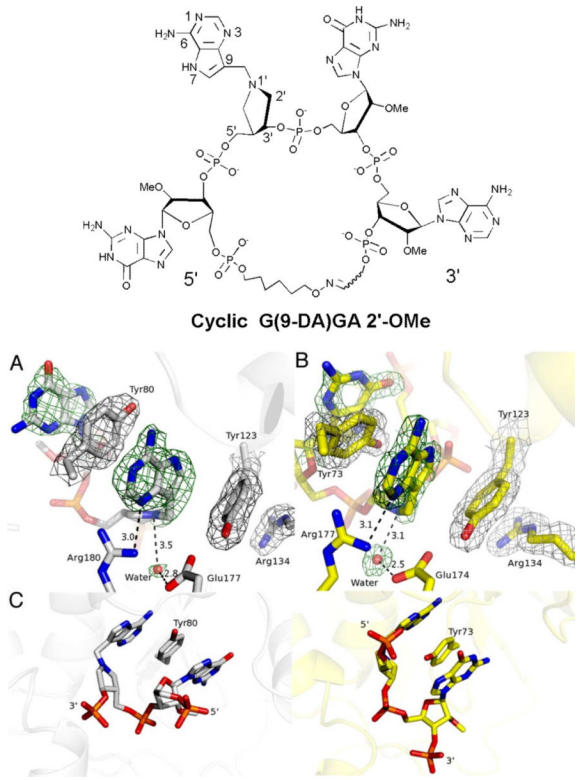

Fig. 5.

Transition state analogue and structures in complex with ribosome inactivating proteins. (Upper panel) The structure of cyclic G(9-DA)GA 2′-OMe, a transition state analogue mimic for ricin A-chain and saporin L-3. Note the placement of 9-DA between two guanosine residues to mimic the GAG sequence specificity of ribosome inactivating proteins. 9-DA is a transition state mimic of 2′-deoxyadenosine. Atomic numbering for 9-DA follows that for purine nucleosides. (Lower panel) Catalytic site detail of cyclic G(9-DA)GA 2′-OMe bound to (A) ricin A-chain and (B) saporin L-3. In both catalytic sites the 9-DA is involved in π-stacking interactions between two tyrosines. Placing two cationic Arg residues near the adenine position serves to withdraw bonding electrons into the leaving group and a Glu serves as a general base to ionize the water nucleophile. From reference 75 with permission of the publisher.

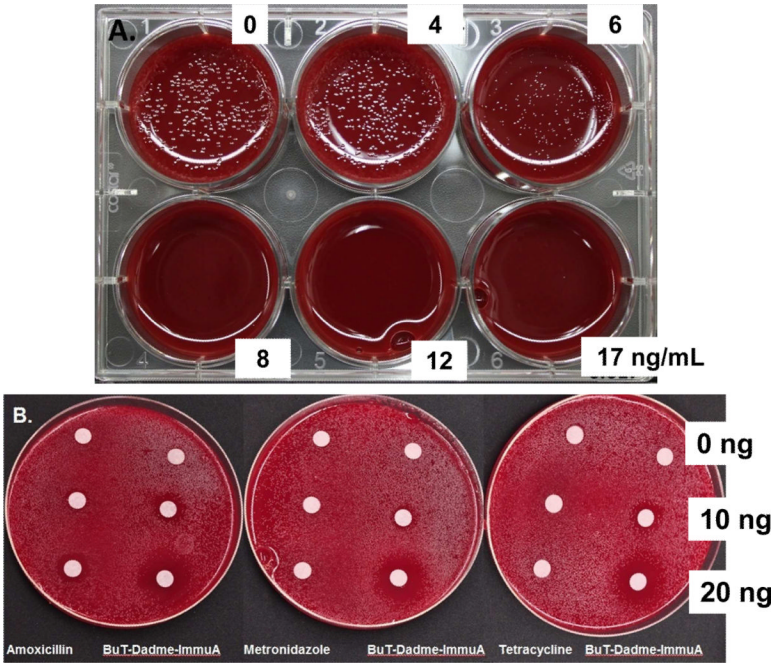

Fig. 6.

Inhibition of *H. pylori* MTAN blocks growth of bacterial cultures. (A) The effect of BuT-DADMe-ImmH (BuT-Dadme-ImmuA; Fig. 4) is shown to have an IC_{90} of less than 8 ng/mL. (B) When compared to the same amounts of amoxicillin, metronidazole or tetracycling, BuT-DADMe-ImmH is more effective. From reference 90 with permission of the publisher.